First-principles study of lattice dynamics and thermodynamics of osmium under pressure*

Liu Bo(刘 波)[a)], Gu Mu(顾 牡)[a)†], Liu Xiao-Lin(刘小林)[a)],
Huang Shi-Ming(黄世明)[a)], Ni Chen(倪 晨)[a)], Li Ze-Ren(李泽仁)[b)], and Wang Rong-Bo(王荣波)[b)]

[a)] *Shanghai Key Laboratory of Special Artificial Microstructure Materials and Technology, Pohl Institute of Solid State Physics, Tongji University, Shanghai* 200092, *China*

[b)] *Institute of Fluid Physics, China Academy of Engineering Physics, Mianyang* 621900, *China*

(Received 22 December 2008; revised manuscript received 3 July 2009)

We have performed the first-principles linear response calculations of the lattice dynamics, thermal equation of state and thermodynamical properties of hcp Os metal by using the plane-wave pseudopotential method. The thermodynamical properties are deduced from the calculated Helmholtz free energy by taking into account the electronic contribution and lattice vibrational contribution. The phonon frequencies at Gamma point are consistent with experimental values and the dispersion curves at various pressures have been determined. The calculated volume, bulk modulus and their pressure derivatives as a function of temperature are in excellent agreement with the experimental results. The calculated specific heat indicates that the electronic contribution is important not only at very low temperatures but also at high temperatures due to the electronic thermal excitation. The calculated Debye temperature at a very low temperature is in good agreement with experimental values and drops to a constant until 100 K.

Keywords: osmium, lattice dynamics properties, thermodynamics properties

PACC: 6320D, 6370, 7115H, 7120C

1. Introduction

Osmium has drawn considerable attention with its unique mechanical and physical properties. Osmium with the hexagonal close-packed (hcp) structure is the hardest metal element.[1] The bulk modulus measured by Cynn *et al.*[2] is 462 GPa, higher than that of diamond (446 GPa).[3] More recent experiments gave the bulk modulus of 411 GPa by Occelli *et al.*[4] and 395 GPa by Kenichi *et al.*[5] The two latter results are due to the better quasi-hydrostatic conditions which reduce the nonhydrostatic stress by about 9 GPa and more. Therefore, osmium and its compounds (OsC, OsN and OsO_2) are considered as the important superhard candidates.

Some theoretical investigations were performed concerning the bulk modulus and electronic structure under pressure.[6−8] Liang C and Fang Z studied the bulk modulus and electronic structure under pressure considering the effect of spin–orbit coupling.[9]

^{189}Os may become a possible dopant in the temperature measurement by using neutron resonance spectroscopy. For the resonance at 6.71 eV of Os, the cross section at the exact resonance and the ratio of Doppler width at 300 K to the natural width are about 8000 barns and 0.78, respectively (calculated with the data[10,11] based on a simple Einstein model). These two critical quantities[12] are relatively large which means a sharp resonance shape and significant temperature broadening effect can be expected.

Thermal properties of solids depend on their lattice dynamical behaviour. The lattice dynamics properties are well investigated by density functional perturbation theory (DFPT) in the framework of the harmonic approximation. Anharmonic effects can be partly taken into account through calculating the phonon frequencies depending on the crystal volume. This approach is called quasiharmonic approximation which is proved to be an accurate description of the thermodynamic properties of materials.[13−16] The electronic contributions to the thermodynamic properties are easily determined by the conventional density functional theory (DFT).[17−19]

In this paper, we present a theoretical investigation of the lattice dynamics and the thermodynamic properties of the hcp osmium within the framework of quasiharmonic approximation. The thermal equation of state, bulk modulus, phonon dispersion

*Project supported by National Natural Science Associated Foundation (NSAF) of China (Grant No. 10776024), and the Program for Young Excellent Talents in Tongji University.

†Corresponding author. E-mail: mgu@tongji.edu.cn

© 2010 Chinese Physical Society and IOP Publishing Ltd

curves, thermal expansion and Debye temperature of Os metal are reported and discussed.

The paper is organized as follows. Theoretical methods and the calculational details are briefly reviewed in Section 2 and Section 3, respectively. In Section 4, the results of our calculations are presented, discussed and compared to experiments. Finally, our results are summarized in Section 5.

2. Theoretical methods

The Helmholtz free energy F of metal is given by[20]

$$F(V,T) = E_{\rm static}(V) + F_{\rm el}(V,T) + F_{\rm vib}(V,T), \quad (1)$$

where V is the volume, T is the temperature, $E_{\rm static}(V)$ is the static zero-temperature energy, $F_{\rm el}(V,T)$ is the thermal free energy from electronic excitations, and $F_{\rm vib}(V,T)$ is the lattice vibrational contribution (phonon) to the free energy.

The electronic contribution to the free energy is written as

$$F_{\rm el}(V,T) = E_{\rm el}(V,T) - TS_{\rm el}(V,T), \quad (2)$$

where $E_{\rm el}(V,T)$ is the internal energy due to the thermal electronic excitations

$$E_{\rm el}(V,T) = \sum_i f_i\varepsilon_i - \sum_{\varepsilon_i<E_{\rm F}} \varepsilon_i, \quad (3)$$

where f_i is the Fermi–Dirac distribution, ε_i are the energy eigenvalues. $E_{\rm F}$ is Fermi energy.

The electronic entropy takes the form

$$S_{\rm el}(V,T) = -2k_{\rm B}\sum_i [f_i \ln f_i + (1-f_i)\ln(1-f_i)], \quad (4)$$

where $k_{\rm B}$ is the Boltzmann constant.

The electronic free energy $F_{\rm el}$ and electronic entropy $S_{\rm el}$ are determined from the calculated electronic density of states by DFT, assuming that the eigenvalues are temperature-independent for given lattice constants and nuclear positions.

The lattice vibrational contribution to the free energy is determined by

$$F_{\rm vib}(V,T) = k_{\rm B}T\sum_{q,i} \ln\left\{2\sinh\frac{\hbar\omega_i(q,V)}{2k_{\rm B}T}\right\}, \quad (5)$$

where $\hbar\omega_i$ is the phonon energy. The lattice vibrational contribution to the free energy can be obtained by calculating the phonon dispersion relation and the corresponding phonon density of state from the linear response function calculations. The calculations assume that the phonon frequency is only a function of volume and temperature-independent, thus neglect the electron–phonon coupling.

From $F(V,T)$ any other thermodynamical properties can be accessed. The equation of state (EOS) can be given by the definition of pressure

$$P = -\left(\frac{\partial F}{\partial V}\right)_T. \quad (6)$$

The isothermal bulk modulus is defined as

$$B(V,T) = -V\left(\frac{\partial P}{\partial V}\right)_T. \quad (7)$$

The volume thermal expansion coefficient is defined as

$$\alpha_V = \frac{1}{V}\left(\frac{\partial V}{\partial T}\right)_{\rm P} = \frac{1}{B}\left(\frac{\partial P}{\partial T}\right)_V. \quad (8)$$

The vibrational specific heat at constant volume is obtained using the calculated phonon density of state as follows:[21]

$$C_V^{\rm vib} = k_{\rm B}\sum_{q,i}\left(\frac{\hbar\omega_i(q)}{2k_{\rm B}T}\right)^2 {\rm csch}^2\left(\frac{\hbar\omega_i(q)}{2k_{\rm B}T}\right). \quad (9)$$

The electronic specific heat at constant volume can be obtained from

$$C_{\rm V}^{\rm el} = T\frac{\partial S_{\rm el}}{\partial T}. \quad (10)$$

The specific heat at constant pressure can be determined by using the relation[22]

$$C_{\rm P} = C_{\rm V} + \alpha_{\rm V}^2 BVT. \quad (11)$$

3. Calculation details

All calculations are performed using the ABINIT package,[23,24] which is based on pseudopotentials and plane waves. It relies on an efficient fast Fourier transform algorithm[25] for the conversion of wave-functions between real and reciprocal space, on the adaptation to a fixed potential of the band–by–band conjugate gradient method[26] and on a potential-based conjugate-gradient algorithm[27] for the determination of the self-consistent potential. Exchange and correlation are treated in the local density approximation (LDA) or generalized gradient approximation (GGA). The Troullier–Martins pseudopotentials[28] for Os generated by the FHI98PP code[29] are used. The considered valence electrons for Os are $5d^6 6s^2$. Relaxation of

the lattice constants is performed using the Broyden–Fletcher–Goldfarb–Shanno algorithm until the maximum component of force acting on any atoms is less than 1 mhartree/bohr.

Lattice dynamics properties (phonon frequency and dispersion relation) are obtained as second-order derivatives of the total energy with respect to an external electric field or to atomic displacements within the framework of DFPT.[30−32] The linear response method allows the calculation of the dynamical matrix at arbitrary q vectors. The force constants are extracted from a Fourier transform of the dynamical matrices obtained for a grid in the Brillouin zone (BZ). They are later employed to obtain the phonon frequencies at arbitrary points in reciprocal space and the phonon-dispersion relations by interpolation. The phonon density of states is also calculated using these force constants. The wave functions are expanded in plane waves up to a kinetic energy cutoff of 30 Ha. The BZ is sampled by a 16×16×12 Monkhorst–Pack mesh[33] of k points. Convergence tests show that the BZ sampling and the kinetic energy cutoff are sufficient to guarantee an excellent convergence within 1 cm^{-1} for the calculated phonon frequencies. The phonon band structures based on interatomic force constants are obtained by Fourier interpolation. The spin–orbit coupling may have effect on the calculated results such as bulk modulus and band structure,[9] however, the pseudopotential used in the present calculations is not allowed to include the spin–orbit coupling.

4. Results and discussions

4.1. Static lattice

Table 1 lists the calculated lattice constants and bulk modulus of Os at 0 K as well as the experimental values. The lattice constants of LDA show more consistency with the experimental values[5] in comparison with the GGA results, which is often found in heavy $5d$ elements.[7,34] The following calculations are performed with LDA. The bulk modulus B_0 and their pressure derivatives B_0' can be obtained by fitting the calculated EOS (P–V curve). We try to fit them with Vinet and Birch–Murnaghan EOS which are described below. In the third-order Birch–Murnaghan EOS, the pressure is given by[35]

$$P(V,T) = \frac{3}{2}B_0\left[\left(\frac{1}{x}\right)^{7/3} - \left(\frac{1}{x}\right)^{5/3}\right] \times \left\{1 + \frac{3}{4}(B_0' - 4)\left[\left(\frac{1}{x}\right)^{2/3} - 1\right]\right\}. \quad (12)$$

In the Vinet EOS, the free energy can be expressed as[36]

$$F(V,T) = F_0(T) + \frac{9B_0(T)V_0(T)}{\xi^2} \times \{1 + [\xi(1-x) - 1]\exp[\xi(1-x)]\}, \quad (13)$$

and the pressure can be obtained as

$$P(V,T) = \left\{\frac{3B_0(T)(1-x)}{x^2}\right\}\exp[\xi(1-x)], \quad (14)$$

where $x = [V(T)/V_0(T)]^{1/3}$, $\xi = \frac{3}{2}(B_0' - 1)$, $B_0' = (\partial B(T)/\partial P)_0$, $F_0(T)$ and $V_0(T)$ are the zero pressure equilibrium free energy and volume, respectively. The subscript 0 represents the values at 0 GPa pressure.

Table 1. The calculated lattice parameters a_0 (Å), c/a, bulk moduli B_0 (GPa), and their pressure derivatives B_0' of Os at 0 K. The Vinet and Birch–Murnaghan (B–M) equations of state are used to fit the calculated P–V curves (1 Å=0.1 nm).

		LDA	GGA	Exp.
a (Å)		2.749	2.753	2.735 (Ref. [5])
c/a		1.580	1.581	1.579 (Ref. [5])
B_0	B–M EOS	435.59	400.26	462(12) (Ref. [2])
	Vinet EOS	433.03	397.58	411±6 (Ref. [4]) 395(15) (Ref. [5])
B_0'	B–M EOS	4.65	4.67	2.4(0.5) (Ref. [2])
	Vinet EOS	4.85	4.88	4.0±0.2 (Ref. [4]) 4.5(5) (Ref. [5])

The EOS (P–V curve) of Os with LDA calculation is presented in Fig. 1. The result is well consistent with the experimental values.[4,5] The differences of B and B_0' with two EOS fittings is less than 1%.

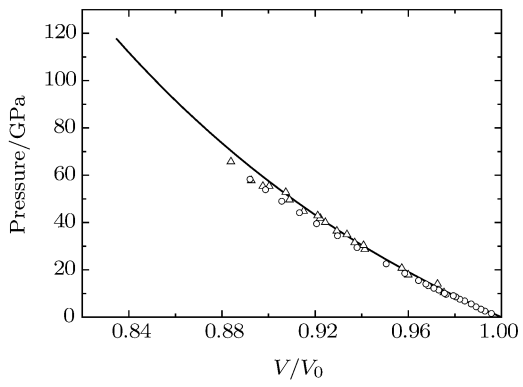


Fig. 1. Equation of state (P–V curve) of Os with LDA calculation. Theoretical values are shown by solid line. The experimental results are marked with open triangles (Ref. [4]) and circles (Ref. [5]).

4.2. Lattice dynamics

We first calculate the phonon energy at the zone center (Γ point). Since there are two atoms in the primitive cell, there are a total of 6 modes of vibration. The theoretical group analysis predicts the following irreducible representations of acoustical and optical zone-centre modes: $\Gamma_{\rm aco} = A_{2u} \oplus E_{1u}$ for acoustic modes, and $\Gamma_{\rm opt} = E_{2g} \oplus B_{1g}$ for optical modes. Only the transverse optical phonon mode of E_{2g} is Raman active, which corresponds to the displacement of two sublattices in a basal plane of a crystal. The optical phonon mode of B_{1g} is a silent mode. Our calculated phonon energy of E_{2g} at 0 K and 0 GPa is 168.3 cm^{-1} which is good agreement with the experimental values[37] of 168.5 and 171.7 cm^{-1} at 10 K and 0 GPa. The calculated E_{2g} phonon energy dependent on the pressure is presented in Fig. 2.

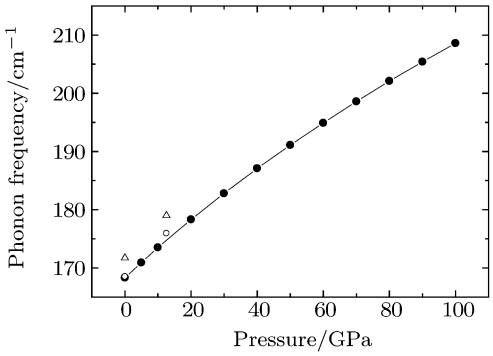


Fig. 2. Calculated phonon energy of Os versus pressure at 0 K (solid circles), together with the experimental Raman measurement at 10 K (open circles and open triangles represent the excitation wavelengths of 514 nm and 647 nm, respectively[38]).

The pressure dependence of the Raman frequency can be described well by a second-order polynomial $\omega(P) = \omega_0 + \alpha P + \beta P^2$ with $\omega_0 = 168.4(1)$ cm^{-1}, $\alpha = 0.507(4)$ cm^{-1}/GPa and $\beta = -0.00407(4)$ cm^{-1}/GPa^2 which can be compared with the experimental results[37] (at 300 K) of $\omega_0 = 164.9(1)$ cm^{-1}, $\alpha = 0.73(5)$ cm^{-1}/GPa and $\beta = -0.008(3)$ cm^{-1}/GPa^2. Our calculations are also consistent with other theoretically calculations.[38] However, it is should be mentioned that in our calculation, the electron–phonon interaction is ignored. Somewhat higher phonon frequencies should be expected if we take into account the electron–phonon interaction which gives evident effect only at low temperature but vanishes at room temperature due to the smearing of electronic self-energy effects. The phonon dispersion curves of Os along several symmetry directions in the hexagonal Brillouin-zone at different pressures (lattice constants) are displayed in Fig. 3. In general, the calculated phonon dispersion curves of Os are similar to those of other hcp metals.[39] With the increasing pressure, the phonon frequencies show

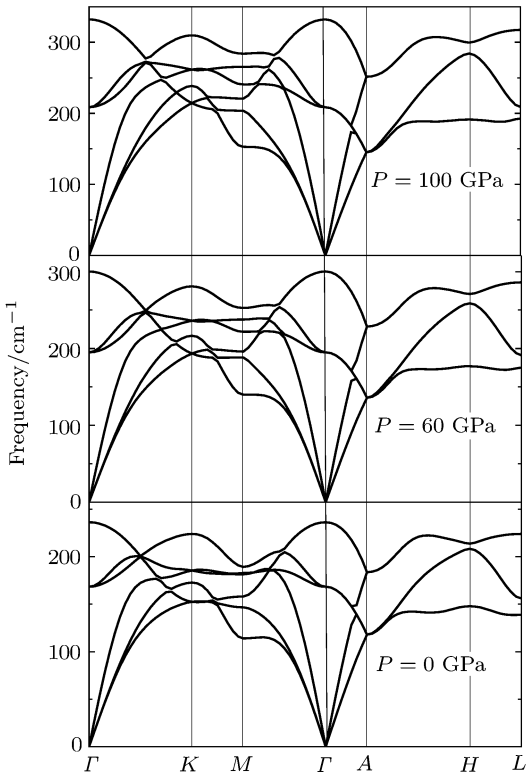


Fig. 3. The phonon dispersion curves of Os along several symmetry directions at different pressures (lattice constants).

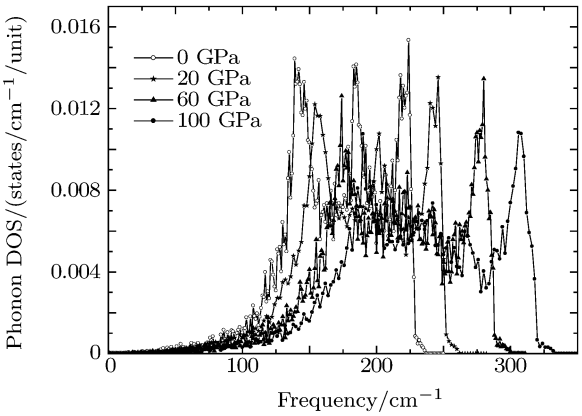


Fig. 4. The lattice vibrational density of states of Os at different pressures.

a positive frequency–pressure dependence without unusual softening, which is consistent with the previous calculation.[38] The longitudinal optic phonons are almost degenerate at M point (1/2,0,0) at 0 GPa pres-

sure, but the degeneration disappears at high pressures. We do not find the anomalous behaviour of longitudinal branch along [001] (Γ–A) direction, which was reported on hcp Ru.[40] The vibrational densities of states at various pressures are illustrated in Fig. 4. With the increase of pressure, the phonon frequencies show a strong increase.

4.3. Thermodynamics properties

After calculating the electronic and phonon structures, the Helmholtz free energy F as a function of volume at various temperatures, presented in Fig. 5, can be constructed using Eq. (1). The parameters of B_0, B_0' and V_0 as a function of temperature obtained by fitting Helmholtz free energy to the Vinet EOS

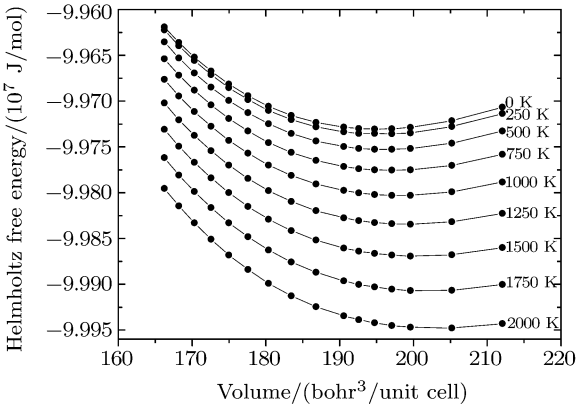


Fig. 5. Volume dependence of the Helmholtz free energy of Os at various temperatures.

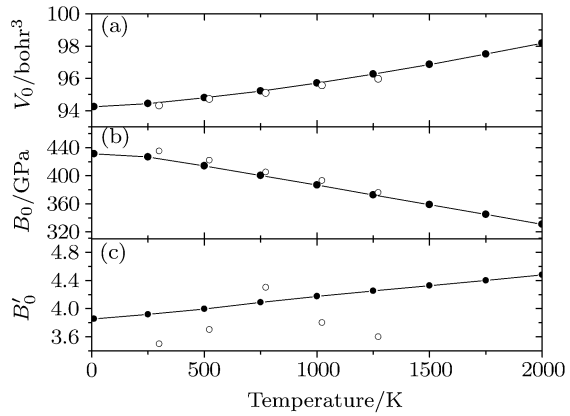


Fig. 6. B_0, B_0' and V_0 as a function of temperature obtained by fitting Helmholtz free energy to the Vinet EOS. The open circles represent the experimental values in Ref. [1].

of Eq. (13) are shown in Fig. 6. The volume shows the normal thermal expansion; and the bulk modulus decreases with temperature. The calculated values are reasonable agreement with the experimental values by the synchrotron x-ray diffraction.[1] These trends are similar to iron.[15] We then can plot the thermal equation of state at temperatures between 0 and 2000 K with the fitted parameters according to Eq. (14), as shown in Fig. 7. The isothermal bulk modulus as a function of pressure is plotted in Fig. 8

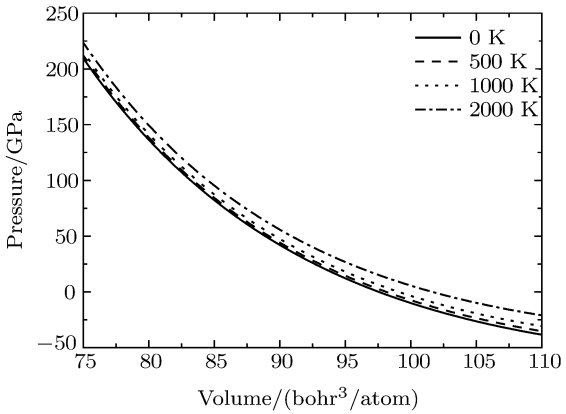


Fig. 7. Calculated thermal equation of state of Os at different temperatures between 0–2000 K.

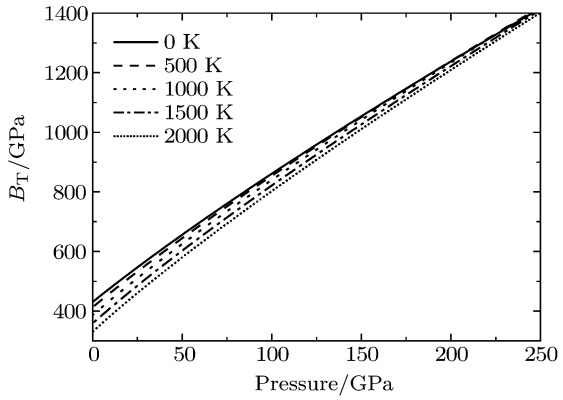


Fig. 8. Isothermal bulk modulus as a function of pressure of Os within temperature range 0–2000 K.

according to Eq. (7). It is found that the bulk modulus increases almost linearly with pressure and the slope also increases with temperature. Figure 9 shows the volume thermal expansion coefficient at various pressures which can be obtained using Eq. (8). We calculate the volume thermal expansion coefficient of Os at different pressures, as shown in Fig. 9. The experimental linear thermal expansion coefficient of hcp Os at ambient pressure is $\alpha_a = (4.0 - 5.85) \times 10^{-6}$ K^{-1}, $\alpha_c = (5.9 - 8.35) \times 10^{-6}$ K^{-1}, from 323 K to 823 K.[41] So the volume thermal expansion coefficients are 1.39×10^{-5} K^{-1} and 2.0×10^{-5} K^{-1} for 323 K and 823 K, respectively, obtained by the relation of $\alpha = 2\alpha_a + \alpha_c$ for hcp structure. Our calculated results are in good agreement with the experimental

results (shown with the open circles in Fig. 9). The calculated results also indicated that the thermal expansion coefficient drops rapidly with increasing pressure, which is often observed in other metals.[13,15,42]

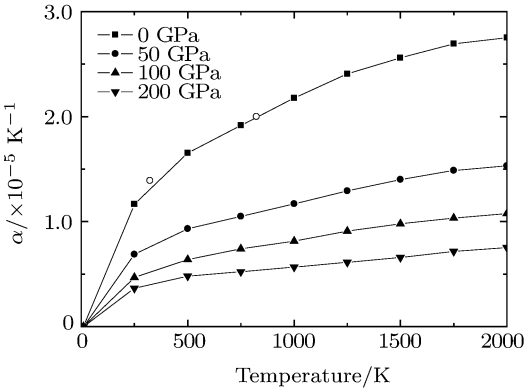


Fig. 9. Volume thermal expansion coefficient of Os at different pressures. The open circles are the experimental values from Ref. [42].

The zero-point motion due to lattice vibration ΔE_0 can be calculated for the internal energy at zero-temperature using the following expression

$$\Delta E_0 = 3nN \int_0^{\omega_{\max}} \frac{\hbar\omega}{2} g(\omega) \mathrm{d}\omega, \qquad (15)$$

where n is the number of atoms per unit cell, N is the number of unit cells, ω is the phonon frequencies, $\omega_{\max}$ is the largest phonon frequency, and $g(\omega)$ is the normalized phonon density of states. The calculated zero-point motions of Os are 3.06 kJ/mol and 4.15 kJ/mol for 0 and 100 GPa pressures, respectively.

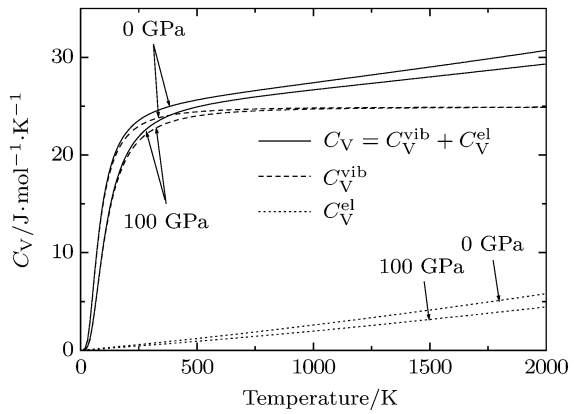


Fig. 10. Temperature dependence of specific heat at constant volume of Os.

The vibrational specific heat at constant volume C_V^{vib} and the electronic contribution to specific heat at constant volume C_V^{el} (shown in Figs. 10 and 11) are calculated using Eqs. (9) and (10), respectively. In the low-temperature limit, C_V^{vib} exhibits the expected T^3 power-law behaviour, and C_V^{el} shows linear increase with temperature. Therefore the low-temperature specific heat at constant volume can be written as $C_V = C_V^{el} + C_V^{vib} = \gamma T + \beta T^3$. We obtain the γ value of 2.33 mJ·mol^{-1}·K^{-2} and 1.79 mJ·mol^{-1}·K^{-2} at the pressures of 0 and 100 GPa, respectively, which can be compared to the experimental value of 2.65 mJ·mol^{-1}·K^{-2} at ambient pressure.[43] Our

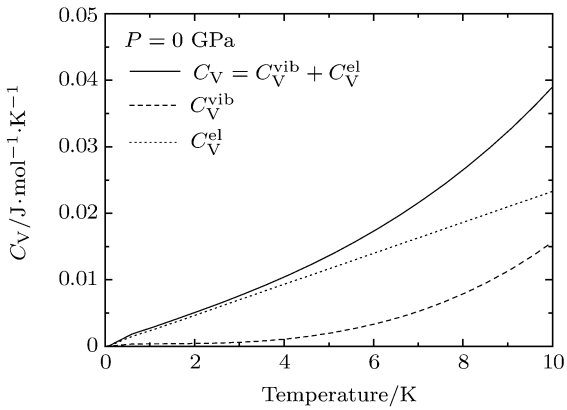


Fig. 11. Temperature dependence of specific heat at constant volume of Os at low temperature of 0–10 K.

theoretical value is underestimated by about 12%, which could be due to the neglect in of the linear anharmonic effect in our calculations. It is also suggested that the electronic specific heat decreases with increasing pressure. The value of β is estimated to be 1.56×10^{-2} mJ·mol^{-1}·K^{-3} and 0.783×10^{-2} mJ·mol^{-1}·K^{-3}, at 0 and 100 GPa, respectively. At high temperatures the classical asymptotic limit is $C_V^{vib} = 3nNk_B = 24.95$ J·mol^{-1}·K^{-1}. While C_V^{el} continually increases with temperature. Therefore, the electronic contribution to the specific heat becomes more important above the temperature at which the lattice vibrational contribution reaches the asymptotic limit. It is very clear that the electronic contribution should be taken into account, especially for the transition metals which have the high electronic density of states (d electrons) near the Fermi level and the large values of γ. The temperature dependence of specific heat at constant pressure C_P can be calculated using Eq. (11). Figure 12 presents the temperature dependence of specific heat at constant volume and pressure. The open circles are the experimental values[44] for C_P. At temperature below 500 K, our calculated values are consistent with the experimental data, while at high temperature the calculated values are higher than the experimental data. The discrepancy between the experimental and calculated C_P is about 6% and

12% at 1000 K and 2000 K, respectively. In fact, our calculated $C_{\rm V}^{\rm vib}$, $C_{\rm V}^{\rm el}$ and the thermal expansion coefficient are all well consistent with experiment, thus the deduced $C_{\rm P}$ is also reasonable. Therefore, the large error may arise from the experiment.

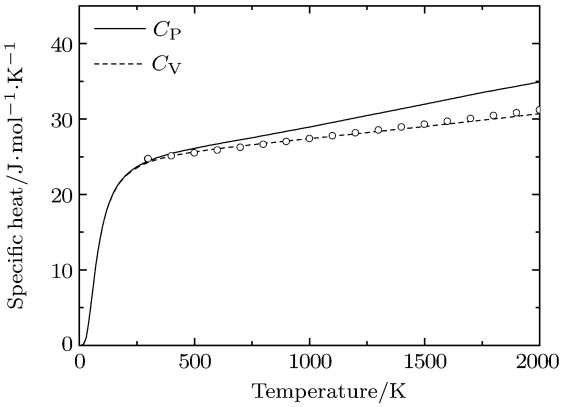


Fig. 12. Temperature dependence of specific heat at constant volume ($C_{\rm V}$) and pressure ($C_{\rm P}$). The open circles are the experimental values for $C_{\rm P}$.

The Debye temperature $\theta_{\rm D}$ (shown in Fig. 13) as a function of temperature at 0 and 100 GPa can be obtained from the calculated volume-constant specific heat by the following equation

$$C_{\rm V}(T/\theta_{\rm D}) = 9Nk_{\rm B}\left(\frac{T}{\theta_{\rm D}}\right)^3 \times \int_0^{\theta_{\rm D}/T} \frac{x^4 {\rm e}^x}{({\rm e}^x-1)^2}{\rm d}x. \quad (16)$$

The $\theta_{\rm D}$ drops with temperature at low temperature and reaches a nearly constant of 325 K and 442 K above 100 K at 0 and 100 GPa, respectively. At low temperature of 7 K, the calculated $\theta_{\rm D}$ is 503 K and 629 K at 0 and 100 GPa, respectively. The $\theta_{\rm D}$ deduced from the experimental standard entropy at 298 K and the experimental low-temperature specific heat at ambient pressure is 320 K and 467 K, respectively.[45] Therefore, the agreement between our calculational and the experimental Debye temperature is excellent.

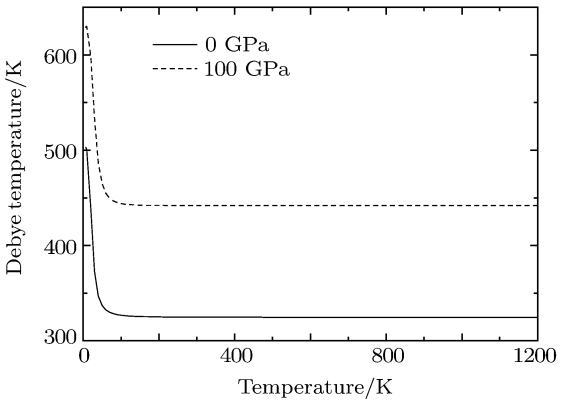


Fig. 13. Calculated Debye temperature of Os as a function of temperature at 0 and 100 GPa.

5. Conclusions

We have preformed the first-principles linear response calculations of the lattice dynamics, thermal equation of state and thermodynamical properties for hcp Os metal. The phonon frequencies at Gamma and dispersion curves at various pressures have been determined. The calculated volume, bulk modulus and their pressure derivatives as a function of temperature are in excellent agreement with experimental values. The thermal expansion coefficient is also calculated and the values at ambient is consistent with experiment. The specific heat at constant volume and constant pressure are calculated by taking into account both electronic contribution and lattice vibrational contribution. The coefficient of low temperature specific heat for electronic contribution γ is consistent with the experimental value. The calculated Debye temperature at low temperature is also in good agreement with experimental values.

References

[1] Voronin G A, Pantea C, Zerda T W, Wang L and Zhao Y 2005 *J. Phys. Chem. Solids* **66** 706

[2] Cynn H, Klepeis J E, Yoo C S and Young D A 2002 *Phys. Rev. Lett.* **88** 135701

[3] Gillet P, Fiquet G, Daniel I, Reynard B and Hanfland M 1999 *Phys. Rev.* B **60** 14660

[4] Occelli F, Farber D L, Badro J, Aracne C M, Teter D M, Hanfland M, Canny B and Couzinet B 2004 *Phys. Rev. Lett.* **93** 095502

[5] Kenichi T 2004 *Phys. Rev.* B **70** 012101

[6] Hebbache M and Zemzemi M 2004 *Phys. Rev.* B **70** 224107

[7] Koudela D, Richter M, Möbius A, Koepernik K and Eschrig H 2006 *Phys. Rev.* B **74** 214103

[8] Zheng J 2005 *Phys. Rev.* B **72** 052105

[9] Liang Y and Fang Z 2006 *J. Phys.: Condens. Mat.* **18** 8749

[10] Kittel C 1995 *Introduction to Solid State Physics* Wiley Text Books 7th ed. (New York: John Wiley & Sons) p. 120

[11] Mughabghab S F 1984 *Neutron Cross Sections* Vol. 1 Part B (New York: Academic Press Inc.)

[12] Fowler P H and Taylor A D 1987 *Rutherford Appleton Laboratory* RAL-87-056

[13] Bouchet J, Jollet F and Zérah G 2006 *Phys. Rev.* B **74** 134304
[14] Rignanese G M, Michenaud J P and Gonze X 1996 *Phys. Rev.* B **53** 4488
[15] Sha X and Cohen R E 2006 *Phys. Rev.* B **73** 104303
[16] Huang G Q, Miao R D and Tian M 2008 *Acta Phys. Sin.* **57** 3709 (in Chinese)
[17] Ai Q, Chen X R, Cheng Y and Fu Z J 2008 *Chin. Phys.* B **7** 2639
[18] Cui H L, Ji G F, Xiao F, Meng C M, Song Z F, Zhang Y L and Zhao F 2009 *Acta Phys. Sin.* **58** 4103 (in Chinese)
[19] Hou Y and Yuan J M 2007 *Acta Phys. Sin.* **56** 3458 (in Chinese)
[20] Wasserman E, Stixrude L and Cohen R E 1996 *Phys. Rev.* B **53** 8296
[21] Lee C and Gonze X 1995 *Phys. Rev.* B **51** 8610
[22] Callen H B 1985 *Thermodynamics and an Introduction to Thermostatistics* (New York: John Wiley & Sons) p. 189
[23] The ABINIT code is a common project of the Université Catholique de Louvain and other contributors (URL http://www.abinit.org)
[24] Gonze X, Beuken J M, Caracas R, Detraux F, Fuchs M, Rignanese G M, Sindic L, Verstraete M, Zerah G, Jollet F, Torrent M, Roy A, Mikami M, Ghosez P, Raty J Y and Allan D C 2002 *Comput. Mater. Sci.* **25** 478
[25] Goedecker S 1997 *SIAM J. Sci. Comput.* **18** 1605
[26] Payne M C, Teter M P, Allan D C, Arias T A and Joannopoulos J D 1992 *Rev. Mod. Phys.* **64** 1045
[27] Gonze X 1996 *Phys. Rev.* B **54** 4383
[28] Troullier N and Martins J L 1991 *Phys. Rev.* B **43** 1993
[29] Fuchs M and Scheffler M 1999 *Comput. Phys. Commun.* **119** 67
[30] Gonze X 1997 *Phys. Rev.* B **55** 10337
[31] Gonze X, Allan D C and Teter M P 1992 *Phys. Rev. Lett.* **68** 3603
[32] Gonze X and Lee C 1997 *Phys. Rev.* B **55** 10355
[33] Monkhorst H J and Pack J D 1976 *Phys. Rev.* B **13** 5188
[34] Eschrig H, Richter M and Opahle I 2004 *Relativistic Electronic Structure Theory* — Part II: *Applications* ed. Schwerdtfeger P (Amsterdam: Elsevier) pp. 723–776
[35] Birch F 1947 *Phys. Rev.* **71** 809
[36] Vinet P, Rose J H, Ferrante J and Smith J R 1989 *J. Phys.: Condens. Mat.* **1** 1941
[37] Ponosov Y S, Loa I, Mogilenskikh V E and Syassen K 2005 *Phys. Rev.* B **71** 220301(R)
[38] Ma Y, Cui T, Zhang L, Xie Y, Zou G, Tse J S, Gao X and Klug D D 2005 *Phys. Rev.* B **72** 174103
[39] Wakabayashi N, Scherm R H and Smith H G 1982 *Phys. Rev.* B **25** 5122
[40] Heid R, Pintschovius L, Reichardt W and Bohnen K P 2000 *Phys. Rev.* B **61** 12059
[41] Childs B G 1953 *Rev. Mod. Phys.* **25** 665
[42] Cohen R E and Gülseren O 2001 *Phys. Rev.* B **63** 224101
[43] Naumov V N 1994 *Phys. Rev.* B **49** 13247
[44] Barin I 1995 *Thermochemical Data of Pure Substances* 3rd ed. (Weinheim: Wiley-VCH Verlag GmbH & Co.)
[45] Guillermet A F and Grimvall G 1989 *Phys. Rev.* B **40** 1521